geophysical prospecting

QUAERE ET INVENIES

European Association
of Exploration Geophysicists

1991 Publication Schedule

Volume 39:1 January
Volume 39:2 February
Volume 39:3 April
Volume 39:4 May
Volume 39:5 July
Volume 39:6 August
Volume 39:7 October
Volume 39:8 November

GPPRAR39 (3) 293–452 (1991)
ISSN 0016-8025
Volume 39 Number 3
April 1991

Geophysical Prospecting is published for the European Association of Exploration Geophysicists by Blackwell Scientific Publications Ltd, Oxford, U.K. The Association, the Editor, and the publisher cannot be held responsible for the opinions given and the statements made in the articles published in the journal, the responsibility resting with the authors. The use of registered trade or service names, etc., in this publication, even without specific reference to such registration, cannot be construed to mean that these names are exempt from the relevant protective regulations.

Subscription information *Geophysical Prospecting* is published eight times per year (1 volume per annum) and the subscription prices for 1991 are £149.50 (U.K.), £180.00 (Overseas except North America), $328.50 (U.S.A. and Canada), in all cases post free. Orders for current subscriptions and back issues should be sent to Journal Subscriptions Department, Marston Book Services, P.O. Box 87, Oxford, U.K. (telephone no. 0865 791197, Telex 837 515 Mardis G, Fax 0865 721205); all other business correspondence, including orders for offprints and advertising space, should be addressed to Blackwell Scientific Publications Ltd, Osney Mead, Oxford OX2 0EL, U.K. (telephone no. 0865 240201, Telex 83355 Medbok G, Fax 0865 721205).

Despatch The Journal is despatched within Europe by surface mail, to other continents by various forms of air-speeded delivery: to the U.S.A. by air freight for forwarding by second class post, to India by air freight for guaranteed local delivery, and to all other countries by Accelerated Surface Post. Second class postage paid at New York, N.Y. Post Master, send address changes to Geophysical Prospecting, c/o Mercury Airfreight International Inc., 2323 Randolph Avenue, Avenel, NJ 07001, U.S.A.

Previous issues For volumes published between 1953 and 1985 please contact Messrs Swets & Zeitlinger B.V., Backsets Department, P.O. Box 810, 2160 SZ Lisse, The Netherlands.

Geophysical Prospecting **39**, 293–312, 1991

ADAPTIVE PICKING OF REFRACTED FIRST ARRIVALS[1]

UMBERTO SPAGNOLINI[2]

ABSTRACT

SPAGNOLINI, U. 1991. Adaptive picking of refracted first arrivals. *Geophysical Prospecting* **39**, 293–312.

Static correction computations require knowledge of the refracted traveltimes. Zero-phase wavelet sources cannot be picked reliably when incoherent picking techniques are used.

Assuming a complex convolutional model for Vibroseis, a coherent picking technique based on the matched filter is described. In order to match the filter to the first arrival wavelet an adaptive algorithm is used. This allows the filter to change both with shot and offset so that all the properties of matched filtering such as improvement of S/N and resolution can be exploited. Incoherent picking is used before coherent picking to improve the convergence of adaptive picking.

INTRODUCTION

Fully automatic procedures for the computation of static corrections often require algorithms that are able to exploit the multiple coverage supplied by the seismic survey. These, in turn, require reliable algorithms for automatic picking of refracted first arrivals; in fact, one of the most relevant problems in refracted arrivals inversion is the accurate estimation of their traveltimes. A simple algorithm for incoherent picking based on the abrupt deviation of energy or the moving energy ratio (MER) measured along the trace is presented. This technique behaves poorly whenever the source wavelet is zero-phase or when the signal-to-noise ratio (S/N) is low. More reliable results are obtained for Vibroseis sources using a coherent technique based on wavelet recognition.

Firstly a convolutional model of the Vibroseis signal that represents the mixed-phase wavelet is given and then a method for coherent picking based on adaptive matched filtering is described. This technique provides the maximum resolution allowed by the signal bandwidth and improves the S/N. The complex signal, which

[1] Based on a paper read at the 50th EAEG meeting, The Hague, June 1988; manuscript received February 1989, revision accepted August 1990.

[2] Dipartimento di Elettronica, Politecnico di Milano, Piazza Leonardo da Vinci 32, I-20133 Milano, Italy.

is the output of a filter matched to the first arrival, is calculated together with its instantaneous amplitude and phase. Owing to spectral attenuation due to absorption and the minimum-phase property of the medium, the matched filter changes in order to obtain a space-variant matched filter.

Secondly an adaptive algorithm for picking is described. The instantaneous amplitudes at.the peaks control the adaptation rate of the algorithm, thus allowing, when possible, variations of the filter spectrum and phase with both shot and offset.

Finally, incoherent picking is compared with coherent picking. Incoherent picking is also used to locate the computationally time-consuming coherent algorithm on the first arrival.

Picking of First Arrival

The computation of static corrections requires knowledge of the times of the refracted first arrivals. If the assumption that the refracted path time is the minimum path time were true, it would be possible to find the refracted time by simply computing the first arrival time. Thus in Fig. 1, for shot point y and offset x, the refracted time $T_{SACR}(x, y)$ is less than the reflected time $T_{SBR}(x, y)$, i.e.

$$T_{SACR}(x, y) < T_{SBR}(x, y). \qquad (1)$$

For a single flat layer model of average depth h, this is satisfied only if the offset x is greater than the crossover offset given by

$$x_{\text{crossover}} \simeq \frac{4hV_1V_2}{V_2^2 - V_1^2}. \qquad (2)$$

In a multilayer model, the problem of finding the arrival associated with each layer is more complicated and a solution to this problem for a two-layer model using a first arrival predictor that locates the adaptive algorithm for the first arrival is suggested. For a single-layer model, the first arrival time is the sum of the refracted time and unavoidable errors, i.e.

$$t_{\text{first arrival}} = T_{SACR}(x, y) + \Delta\tau_{\text{picking error}}. \qquad (3)$$

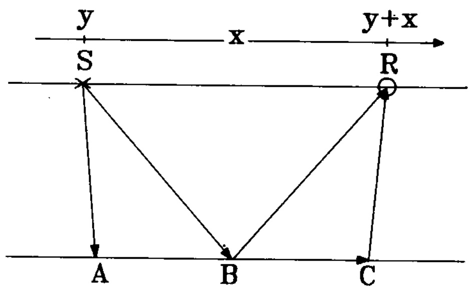

FIG. 1. Simple one-layer model for reflected and refracted path.

The picking error is due to two main contributions, i.e.

$$\Delta\tau_{\text{picking error}} = \Delta\tau_{\text{noise}} + \Delta\tau_{\text{modelling error}}. \qquad (4)$$

$\Delta\tau_{\text{noise}}$ is the time error due to low S/N; it has, generally, zero mean value and unknown probability density. Before picking, we must obtain a model of the first arrival wavelet and we have also to keep in mind that an incorrect evaluation of its spectrum or phase can lead to a systematic picking error. This is the error due to incorrect modelling of the first arrival wavelet or $\Delta\tau_{\text{modelling error}}$.

In Vibroseis picking, a technique that exploits the nearly zero-phase property of the wavelet must be used. $\Delta\tau_{\text{modelling error}} < 0$ can be accepted using a suitable minimum-phase wavelet technique.

Incoherent picking techniques are usually based on the estimation of that time at which the signal power or some other statistical property of the trace changes abruptly. This technique is very easy to use and implement but, since there is only a statistical model of the first arrival wavelet, the average squared time error due to noise $(\overline{\Delta\tau^2_{\text{noise}}})$ is high and the average modelling time error $(\overline{\Delta\tau_{\text{modelling error}}})$ is usually non-zero. Alternatively there is another way to detect the first arrival, which consists of searching for the first arrival wavelet by comparing the trace with a reference wavelet. This technique is the one that uses wavelet recognition algorithms and is called the coherent picking technique. The algorithm developed uses a model of the first arrival wavelet and a suitable choice allows $\overline{\Delta\tau_{\text{modelling error}}} \simeq 0$; $\overline{\Delta\tau^2_{\text{noise}}}$ is also low for a suitable matched filter.

MER Incoherent Picking

Let us consider a sampled trace $s(n)$ and define two power functions, Backward power $B(k)$ and Forward power $F(k)$ over L_B and L_F samples respectively, weighted with symmetrical windows $w(n)$, i.e. $w(-n) = w(n)$:

$$B(k) = \frac{\sum_{n=k-L_B}^{k-1} [w(n + L_B/2 - k)s(n)]^2}{L_B} \qquad (5)$$

and

$$F(k) = \frac{\sum_{n=k+1}^{k+L_F} [w(n - L_F/2 - k)s(n)]^2}{L_F}. \qquad (6)$$

We define a new function, MER (moving energy ratio), given by

$$MER(k) = \frac{F(k)}{B(k)}. \qquad (7)$$

Amongst the properties of this function, we are interested in that which gives the first arrival time (k_1) where

$$MER(k_1) > MER(k), \quad \text{where } k \neq k_1. \qquad (8)$$

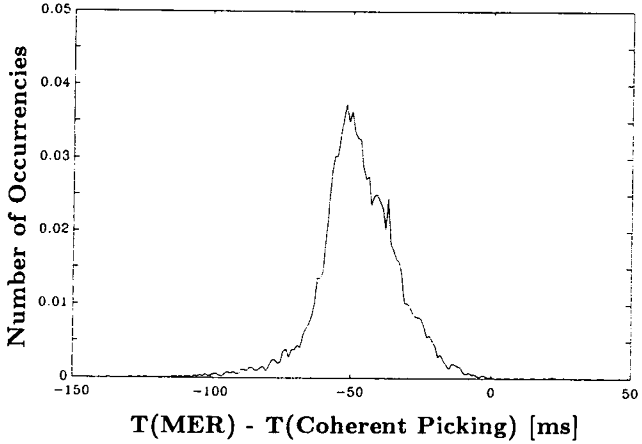

FIG. 2. Histogram of relative time error for a Vibroseis line (Line 1): $[t_{\mathrm{MER}} - t_{\mathrm{Coherent\ Picking}}]$.

This algorithm is similar to the one introduced by Coppens (1985). Due to the nearly zero-phase of the Vibroseis wavelet, MER picking has the systematic error shown in Fig. 2, i.e. $\Delta\tau_{\mathrm{modelling\ error}} \simeq -50$ ms.

Coherent Picking

It would be easy to find the first arrival wavelet for an ideal medium with no absorption and a pure delay response as shown in Fig. 1. In this case, it would be sufficient to find the first maximum of the trace, to discover the first arrival time, but unfortunately, the coherent picking technique has no such simple solution.

There are several reasons why the earth's response is much more complex than a simple delay. Let us consider some of the most important effects. Firstly, the acoustic waves in a semi-infinite medium propagate spherically from the source and this reduces their amplitude with offset by almost $x^{-1/2}$ (Waters 1978); secondly, the transmitting medium is a minimum-phase low-pass filter due to absorption (Aki and Richards 1980); and thirdly, the geometrical optic approximation of the wave path is usually a greatly simplified version of forward modelling (Woodward and Rocca 1988). Another difficulty arises from the low S/N of recorded traces which reduces the accuracy of wavelet modelling. Coherent picking needs a model of first arrival wavelets in order to be used in a wavelet recognition technique. It is convenient first to find a way to parametrize the received wavelet and then to use these parameters for the wavelet recognition algorithm.

Single-layer signal model for coherent picking

Let us consider a single wavelet trace from a single-layer model with a refracted first arrival. The source wavelet $w_0(t)$ will be a zero-phase wavelet. Because of the

undesirable effects previously mentioned, the arrival wavelet is a mixed-phase wavelet with noise superimposed on it. Since only the analytical wavelet of a given real wavelet (Papoulis 1984; Taner, Koehler and Sheriff 1979) is considered, let us first discuss the Hilbert transform. Given a real signal $w(t)$, the output $\hat{w}(t)$ of a filter with an impulse response $1/\pi t$ is given by

$$\hat{w}(t) = w(t) * \left(\frac{1}{\pi t}\right) \leftrightarrow W(\omega)[-\mathrm{j}\ \mathrm{sgn}\ (\omega)]. \tag{9}$$

This signal, denoted by $\hat{w}(t)$, is known as the Hilbert transform of $w(t)$ (Papoulis 1984), while the filter is usually known as the quadrature filter because its response to $\cos(\omega t)$ equals $\sin(\omega t)$. The analytical signal of $w(t)$ is defined as the signal

$$\phi(t) = w(t) + \mathrm{j}\hat{w}(t). \tag{10}$$

It is meaningful to represent the analytical signal with its amplitude and phase by

$$\phi(t) = |\phi(t)|\ \mathrm{e}^{\mathrm{j}\theta(t)},$$

where $|\phi(t)|$ is the complex envelope of the real signal $w(t)$ and $\theta(t)$ is the instantaneous phase of the analytical signal.

The analytical trace of the single layer with the single refracted wavelet is

$$s(x, y, t) = r(x, y)w[x, y, t - \tau(x, y)]\mathrm{e}^{\mathrm{j}\theta(x, y, t)}, \tag{11}$$

where $r(x, y)$ is the refracted arrival amplitude for y and x; $w(x, y, t)$ is the analytical recorded wavelet which is mixed phase; and the phase $\theta(x, y, t)$ is a phase shift, generally time-dependent. In order to simplify the model, let us assume that the recorded wavelet is still a zero-phase wavelet $w_0(x, y, t)$ and that the phase shift is time-independent. This means that

$$s(x, y, t) \simeq r(x, y)w_0[x, y, t - \tau(x, y)]\mathrm{e}^{\mathrm{j}\theta(x, y)}, \tag{12}$$

or in the frequency domain (using capital letters for Fourier transformed data)

$$S(x, y, \omega) = |r(x, y)|\ |W_0(x, y, \omega)|\mathrm{e}^{\mathrm{j}[\theta(x, y) - \omega\tau(x, y)]}. \tag{13}$$

Thus the wavelet has its amplitude reduced by $r(x, y)$ and the phase, in the frequency domain, has been expanded into a Taylor's series truncated at the linear term. In this way, the mixed phase that results from the zero-phase wavelet, the minimum-phase characteristic of the absorbing medium, and the interference of other arrivals are all taken into account. When applied to real data, this model for a single recorded wavelet still has some limitations. Firstly, the wavelet is subject to absorption which reduces its bandwidth, and the wavelet also changes with offset. We can assume that the estimation of the zero-phase wavelet on real data allows for the estimation of the wavelet after average absorption. This means that, in the trace model, the best estimate of the average spectrum of a Vibroseis zero-phase wavelet would be the average spectrum of the first arrival wavelets (Fig. 3).

The constant phase shift $\theta(x, y)$ can be used to take into account the mixed phase of the recorded wavelet. The phase of the single wavelet is linearly approximated in the frequency domain. Any change from zero phase to mixed phase could be attributed to (in order of importance): interference, absorption (Angeleri

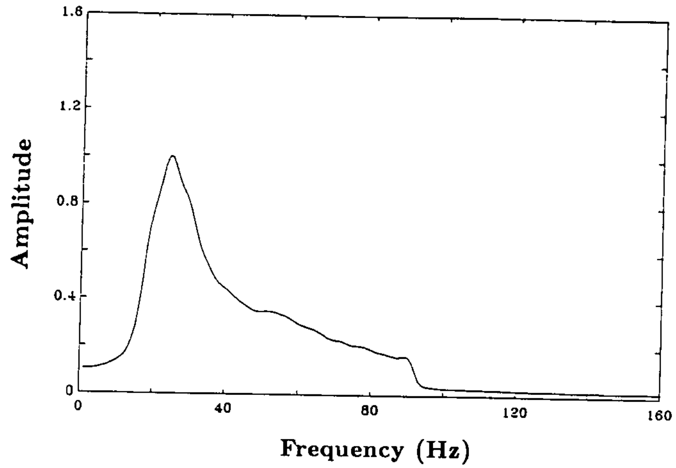

FIG. 3. Spectrum estimation on real Vibroseis data (linear sweep 14–96 Hz of Line 1).

and Loinger 1984); anisotropy, and scattering. A too wide window on the first arrival wavelet gives a less reliable estimation of phase shift because of interference (Angeleri 1983). An abrupt change of first arrival wavelet in a phase versus offset plot could mean strong wavelet interference while absorption can make the phase change slowly (Fig. 4a). The estimated phase shift of the first arrival wavelet of the Vibroseis is not zero but is approximately uniformly distributed between $-\pi$ and $+\pi$ as shown in the phase histogram (Fig. 4b).

The matched filter as wavelet recognizer

In the coherent picking of first arrivals we are interested in finding not only the value of the first arrival time $\tau(x, y)$, but also the values of the amplitude $r(x, y)$ and phase shift $\theta(x, y)$. Due to the multiple coverage, several phase shift, amplitude and first arrival time measurements are available. Since for homogeneous medium, $\theta(x, y)$ and $r(x, y)$ do not change abruptly with offset, these quantities can be used to define a quality factor which could be used in an algorithm that detects and corrects mispicks.

The problem of coherent picking can be summarized as follows: we have to compute, for each trace, the tern $[\tau, r, \theta]_{(x,y)}$ consisting of three terms each dependent on y and x.

Let us consider a single arrival analytical trace $s(t)$. From the model of the single layer signal

$$s(t) \simeq r(x, y)w_0[x, y, t - \tau(x, y)]e^{j\theta(x,y)} + n(t), \tag{14}$$

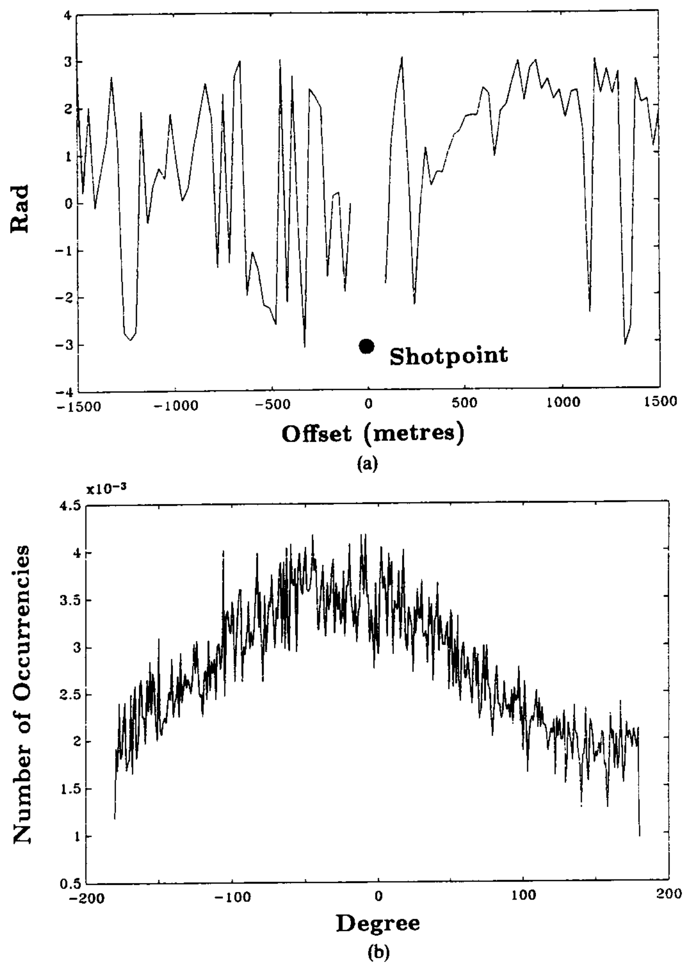

FIG. 4. (a) Example of phase vs. offset on real data (Line 1). (b) Histogram of first arrival phase shift $\theta(x, y)$.

where $n(t)$ is the term that includes noise and the effect of wavelets due to other arrivals that are incompletely reduced by windowing.

Coherent picking uses a wavelet recognition technique based on a complex matched filter applied to the analytical trace. In order to obtain the maximum possible improvement using the matched filter, the filter should be matched to the first arrival wavelet. The impulse response for this filter is

$$h(t) = w_0^*[x, y, t]e^{-j\theta(x,y)} = w_0[x, y, t]e^{-j\theta(x,y)}. \tag{15}$$

The complex output of an ideal matched filter is $g(t)$ given by

$$g(t) = h(t) * s(t) = g_w(t) + g_n(t), \tag{16}$$

where $g_w(t)$ is the filtered first arrival wavelet and $g_n(t)$ is the noise term. The output signal $g(t)$ has well-known properties (Papoulis 1984; Spangnolini 1987) that can be summarized as follows:

(i) $0 \le |g(t)| \le |g(\tau(x, y))| \simeq r(x, y)$, for every $t \neq \tau(x, y)$;
(ii) $\angle[g(\tau(x, y))] \simeq 0$;
(iii) the S/N computed on the first arrival is a maximum given by

$$(\mathrm{S/N})_{\tau(x,y)} = \frac{|g_w(\tau(x, y))|}{g_n^2(t)}.$$

This means that a matched filter allows the coherent computation of the refracted arrival amplitude (i), improving its S/N (iii) even if the wavelet has a phase rotation (ii).

The picking of first arrivals using the coherent algorithm requires matching a filter to the first arrival wavelet. Because of absorption, the first arrival wavelet and the phase shift of the wavelet change with offset, so an algorithm changing the matched filter must be used in order to improve the performance of coherent picking by allowing the filter to be matched to the first arrival wavelet.

The complex matched filter should be space-variant. The adaptive algorithm makes use of all the information available from the data and adapts the filter to the nearest, or just picked, traces for which all the terms $[\tau, r, \theta]_{(x,y)}$ are known.

Adaptive algorithm

The adaptive algorithm allows the complex filter to be matched to the first arrival wavelet by gradually changing bandwidth with offset. Let us consider the filter at the $(N + 1)$th iteration as the contribution of filter $h_N(t)$, term $[\tau, r, \theta]_N$ and trace $s_N(t)$ at the Nth iteration given by

$$h_{N+1}(t) = Adpt[h_N(t), s_N(t), [\tau, r, \theta]_N]. \tag{17}$$

The function $Adpt[\,.\,]$ is the adaptive algorithm which allows for the recursive calculation of the filter to be used at the next step (Fig. 5). Simple functions $Adpt[\,.\,]$ which implement the adaptivity of the matched filter in the frequency domain are considered.

Because the complex envelope of the output of the filter is not sensitive to phase shift, the complex matched filter could be a zero-phase matched filter. In this case $\angle[g(\tau(x, y))] \simeq \theta(x, y)$ for the first arrival wavelet, and a simple spectrum adaptive algorithm is required.

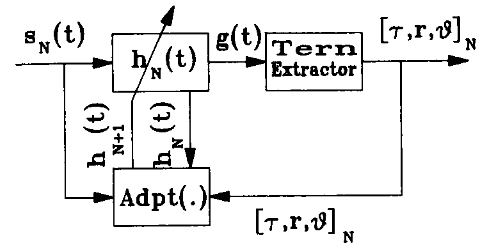

FIG. 5. Block diagram of adaptive matched filter.

The recursive adaptive algorithm that allows only spectrum adaptation has a simple linear equation,

$$|H_{N+1}(\omega)| = c_1|H_N(\omega)| + c_2|S_N(x, y, \omega)|. \tag{18}$$

The coefficients c_1 and c_2 that control the adaptivity have the following restrictions:

1. For stability of the adaptive algorithm, $|c_1| < 1$;
2. c_1 and c_2 are not independent if the energy of the filter is normalized. Normalizing the filter, the complex signal $g(t)$ is the complex correlation between the filter's impulse response and the windowed trace $s_N(x, y, t)$; the following relationship between c_1 and c_2 should hold in order to normalize the energy

$$c_2 = \sqrt{1 + c_1^2[|g(\tau_N)|^2 - 1]} - c_1|g(\tau_N)|. \tag{19}$$

Since $|g(\tau_N)| \le 1$, it follows that

$$c_2 \simeq 1 + \frac{c_1^2}{2}[|g(\tau_N)|^2 - 1] - c_1|g(\tau_N)|. \tag{20}$$

If, as is usual with real data, $|g(\tau_N)| \simeq 1$ then (20) becomes

$$c_2 \simeq 1 - c_1|g(\tau_N)|. \tag{21}$$

In order to control the velocity of the adaptive algorithm to the new wavelet, we should make the coefficient c_2 dependent on the value of the complex envelope computed in the first arrival τ_N, i.e.

$$c_2 = F[|g(\tau_N)|]. \tag{22}$$

The function $F[\,.\,]$ that controls the rate of adaptation has been chosen so that for a low value of argument there is no change, while the change is maximum for the argument close to unity.

In order to fix the maximum rate of change, we should estimate the adaptive algorithm for a simplified model. Let us assume that

$s_N(t) = w_0(t - \hat{\tau})$, i.e. the trace is a delayed zero-phase wavelet for every N, and $h_0(t)$ is the zero-phase filter's wavelet at the first iteration.

It follows that the normalized terms are

$$[\tau, r, \theta]_N = [\hat{\tau}, 1, 0]_N, \text{ for every } N. \tag{23}$$

After N iterations we wish to compute the filter's wavelet as the sum of the residual initialization wavelet $h_0(t)$ and the seismic wavelet $w_0(t)$ that, for this example, is always the same, i.e.

$$h_N(t) = [c_1]^N h_0(t) + \frac{c_2}{1 - c_1} w_0(t). \tag{24}$$

The influence of $h_0(t)$ depends on c_1 and is negligible after few iterations. If the number of memory iterations N_0 is defined as the minimum number of iterations that reduces the influence of the adapting wavelet to 10%, then

$$N_0 = -\frac{1}{\log c_1}. \tag{25}$$

After a large number of iterations with the same adapting wavelet $w_0(t)$, it becomes the dominant wavelet, and using (21)

$$\frac{c_2}{1 - c_1} \simeq \frac{1 - c_1 |g(\tau)|}{1 - c_1} \simeq 1. \tag{26}$$

In the applications to seismic lines an empirical adaptive function that has a cubic trend as shown in Fig. 6 is used. The maximum ($c_2 = F[1] \simeq 0.4$) is chosen so that, for the maximum velocity performance, there are few memory iterations ($N_0 \simeq 4.5$ iterations).

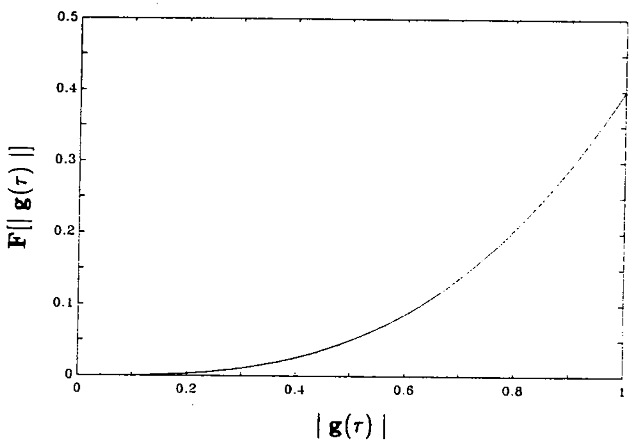

FIG. 6. Cubic adaptivity function.

ADAPTIVE ALGORITHM AND PHASE ESTIMATION

The spectrum adaptivity is suitable for picking the first arrival wavelet because of the insensitivity of the complex envelope to phase shift. A general matched filter for a single-layer model (11) should have its spectrum and phase adapted. This means that a different adaptive algorithm must be used. If the phase parametrization, in the frequency domain, of the first arrival wavelet is simply linear, as the one used here, then phase adaptivity is simply another way to achieve the most accurate phase estimation. In a more complex phase parametrization, the phase adaptivity becomes very important.

The adaptive algorithms that allow phase and spectrum adaptivity for the single-layer model could be divided into joint and disjoint adaptive algorithms. While the first permits the adaptation of phase and spectrum at the same time, the second permits the controlling of the adaptivity of phase and spectrum using different adaptation rates.

In the frequency domain the two algorithms are:

1. The joint adaptive algorithm

$$H_{N+1}(\omega) = c_1 H_N(\omega) + c_2 |S_N(x, y, \omega)| e^{-j\theta_N(x, y)}, \tag{27}$$

where the coefficients c_1 and c_2 have the same meaning as for the adaptive algorithm previously shown. The function that controls the velocity of the adaptive algorithm has the same form as shown in Fig. 6 but in this case it changes the spectrum and phase of the matched filter $h_{N+1}(t)$ simultaneously.

2. The disjoint adaptive algorithm

$$|H_{N+1}(\omega)| = c_1 |H_N(\omega)| + c_2 |S_N(x, y, \omega)|,$$
$$\theta_{N+1} = c_{1_\theta} \theta_N + c_{2_\theta} \theta_N(x, y), \tag{28}$$

where the coefficients c_2 and c_{2_θ} are dependent on two different adaptivity functions, i.e.

$$c_2 = F[|g(\tau_N)|] \tag{29}$$

and

$$c_{2_\theta} = G[|g(\tau_N)|]. \tag{30}$$

Because phase varies more quickly than spectrum, the two adaptivity functions should be different, i.e.

$$0 < F[1] < G[1] \leq 1. \tag{31}$$

Obviously, the adaptive algorithm that allows spectrum adaptation as in (18) is a disjoint algorithm in which $c_{2_\theta} = 0$ and the matched filter phase at the first iteration is zero ($\theta_0 = 0$). A good phase match means that the instantaneous phase computed at the maximum of the envelope of the matched filter (i) should be zero (ii) so that phase matching could be used as a quality factor in adaptive picking. In Fig. 7, two histograms of instantaneous phase with joint (solid) and disjoint (dashed) adaptivity

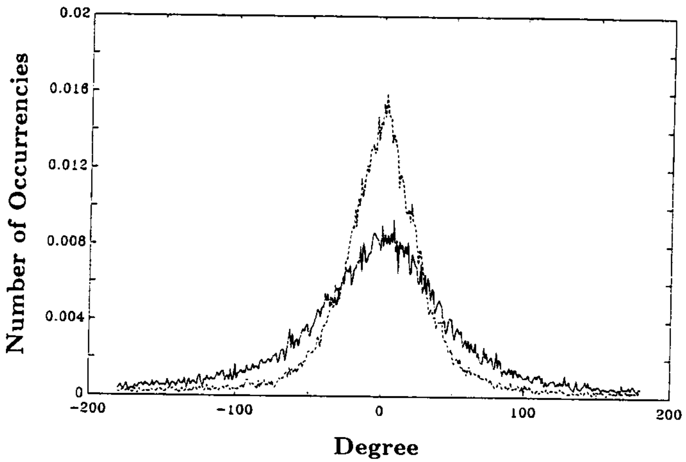

FIG. 7. Phase histogram with disjoint (dashed) and joint (solid) adaptivity.

are shown. The adaptive function $F[|g(\tau(x, y))|]$ is the same for both methods (cubic as in Fig. 6) but the phase adaptivity for the disjoint algorithm is simply

$$c_{2_\theta} = 1.$$

As expected, the disjoint adaptivity gives the best estimation of the phase shift of the first arrival wavelets.

Adaptivity Path

The strategy to adapt the filter in order to get the best estimated wavelet is now outlined.

Obviously the estimated wavelet should be 'a good estimation of the first arrival wavelet'. The optimum path for the adaptive algorithm in shot–receiver space is the path that minimizes the difference between the estimated and the first arrival wavelet.

If the assumptions that the generated seismic wavelet is shot-invariant and that absorption makes the spectrum vary slowly with offset are correct, a single receiver step is the minimum path change that allows the filter to adapt slowly. The optimum adaptivity path is then the one that follows a zigzag path in the shot–receiver plane as shown in Fig. 8.

Multilayer Model for Coherent Picking

Because the recorded trace differs greatly from a single arrival model, we should treat this case separately. As in the case of a single-layer model, let us extend the

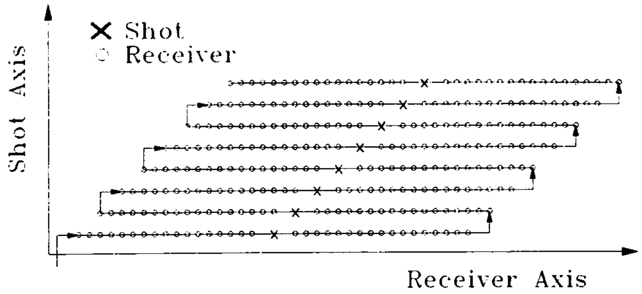

FIG. 8. Adaptivity path in shot–receiver space.

signal modelling to a multilayer model with multiple arrivals. The trace, extending the single-layer model (12) in the same way as the convolutional model does (Goupillaud 1961), should be

$$s(x, y, t) \simeq \sum_i r_i(x, y) w_0[x, y, t - \tau_i(x, y)] e^{j\theta_i(x, y)}. \qquad (32)$$

This means that each refracted and reflected wavelet is modelled in the same way as for the single-layer modelling described before. This permits, where possible, the discovery of the parameters of each wavelet and the characterization of the wavelet by its term $[\tau_i, r_i, \theta_i]_{(x, y)}$. The main problem in coherent picking is to find the term of the first arrival wavelet. The only way to filter the trace for first arrival picking is by windowing the trace before filtering. The two problems that arise are: the locating of the coherent picking on the first arrival and then the choice of a proper window to select only that wavelet.

The resolution depends on the amount of absorption which reduces the wavelet bandwidth with offset; it also depends on the techniques for locating and windowing. To indicate the resolution limits, the following synthetic trace, consisting of two wavelets with Gaussian noise $n(t)$ added, is considered:

$$s(t) = w_0(t) + a w_\theta(t - \tau) + n(t). \qquad (33)$$

The second reflection, delayed by τ, has variable amplitude (0.25–2.0 by steps of 0.25) and a uniformly variable phase shift θ. Noise is chosen so that S/N $\simeq$ 20 dB. Because the complex matched filter picking is independent of the constant phase shift, the average arrival time of the first arrival, normalized to τ to estimate the picking resolution, can be computed using

$$\bar{\tau} = \bar{\tau}(a, \tau) = \frac{E[\tau(a, \tau, \theta)]}{\tau}. \qquad (34)$$

The first resolution test has a wavelet with a flat spectrum from 20–80 Hz and a cosinusoidal transition of 10 Hz at the edges (Fig. 9b). The picking algorithm gives a good resolution of first arrivals shown in Fig. 9a even under the theoretical

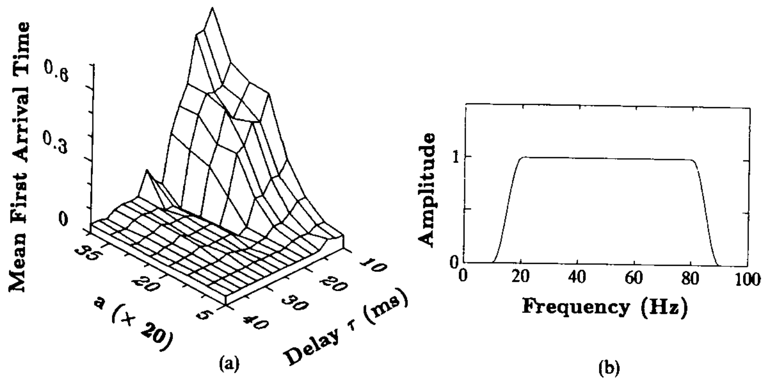

FIG. 9. Synthetic resolution test of coherent picking using two zero-phase wavelets. The second wavelet is delayed by τ, amplified by a and phase-shifted by θ. (a) Normalized first arrival time to the second wavelet delay versus $[\tau, a]$, (scale of a is multiplied by 20); (b) wavelets spectrum.

resolution limit $\tau \simeq 10$ ms. Figure 10 presents the same test with an exponential attenuation applied. The resolution properties are less attractive than those in the flat spectrum case, but this is closer to real data (the spectrum in Fig. 3 is very close to the spectrum of the synthetic traces used for the resolution test).

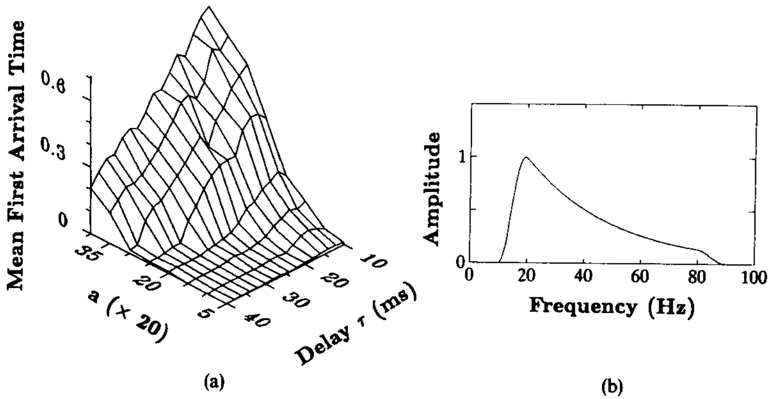

FIG. 10. Synthetic resolution test of coherent picking using two zero-phase wavelets with spectral absorption applied. The second wavelet is delayed by τ, amplified by a and phase-shifted by θ. (a) Normalized first arrival time to the second wavelet delay versus $[\tau, a]$, (scale of a is multiplied by 20); (b) wavelets spectrum (close to the Line 1 average spectrum in Fig. 3).

The mean first arrival diagram shows, for both spectra, that windowing is an important factor in reducing the amplitude of the other wavelets. A deconvolution before picking would improve the resolution as shown in both tests of the mean first arrival time. The use of incoherent picking before coherent picking allows the approximate location of the first arrival so that the first arrival wavelet is well resolved from the other arrivals. For very noisy traces, where incoherent picking fails, a more complicated method of placing the window on the first arrivals should be used. A Gaussian window centred on the estimated first arrival time reduces the effects of close arrivals and, because the resolution is largely dependent on the amplitude of the nearest wavelets, good resolution properties are obtained.

APPLICATIONS OF ADAPTIVE PICKING

The adaptive picking procedure was applied to two Vibroseis seismic lines, Line 1 and Line 2. In order to centre the window on the first arrival an incoherent picking (MER) before the coherent one was used. The window was an double-exponential of 200 ms width (the amplitude between two points of exp (-1) value) centred on the estimated first arrival after being corrected by $\Delta\tau_{\text{modelling error}}$. The quality factors used to demonstrate the improvements of the adaptive technique vs. the MER technique are:

1. The common-shot principle of parallelism (slope congruency).
2. The common-receiver principle of parallelism (time-lag congruency).
3. The rms-error in the wavenumber domain resulting from the static corrections computation in the wavenumber domain (Zanzi and Carlini 1987) (this is a measurement of first arrivals congruency).
4. Congruency of wavelet measured phase.

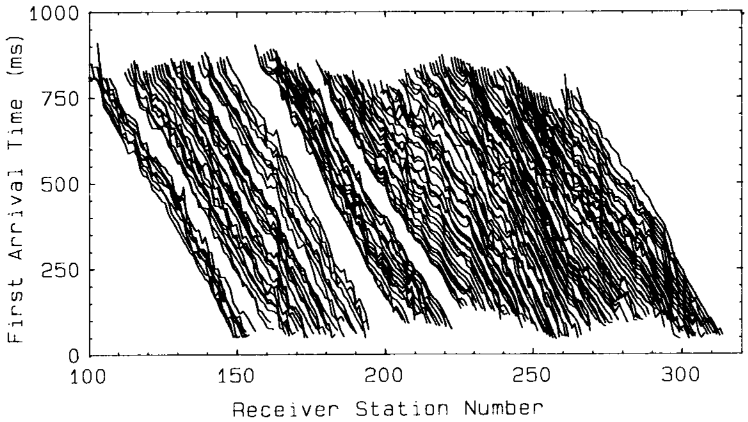

FIG. 11. Traveltime curves of Line 1 with incoherent picking applied.

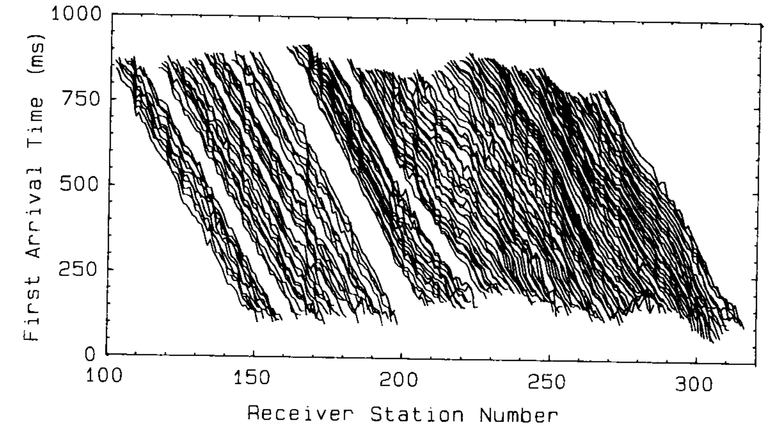

FIG. 12. Traveltime curves of Line 1 with adaptive picking applied.

The traveltime of fully automatic coherent picking (Fig. 11) is compared with that of fully automatic incoherent picking (Fig. 12) and gives the result

$$[\overline{\Delta\tau^2_{\text{noise}}}]_{\text{MER}} \gg [\overline{\Delta\tau^2_{\text{noise}}}]_{\text{Adaptive}}. \qquad (35)$$

The rms-error in the wavenumber domain is reduced with adaptive picking by 3.5–4 dB (Fig. 13a) but the improvement is more evident for high wavenumbers where the percentage of the rms-error reduction is remarkable. Because of the high redundancy of Line 1 data, the values of the refraction statics are mainly the same (Fig. 13b) except for the $\overline{\Delta\tau_{\text{modelling error}}}$ of the MER picking that increases the value of the static d.c. component proportionally. The components at high wavenumbers are improved and an analysis of stack sections, where only refraction static corrections have been applied (Fig. 14), demonstrates better results. Adaptive picking applied to Line 2 was more complicated because incoherent picking before a coherent one was less accurate and led to unavoidable errors. The second refracting layer has much more powerful arrivals than the first one and there was a high probability of confusion between the first and the second layer arrivals. In this case a suitable predictor of first arrival time allows a more reliable location of the first-layer window than the use of the incoherent technique. The traveltime in Fig. 15 demonstrates the accurate results achieved using the fully automatic picking.

Discussion and Conclusions

It has been shown how a coherent picking is preferable to an incoherent measurement of energy (MER). A comparison between the two techniques is summarized in Table 1 after application to real data. Wavelet recognition is performed using a matched filter that changes its spectrum and phase shift with offset since the filter should be matched to the first arrival wavelet.

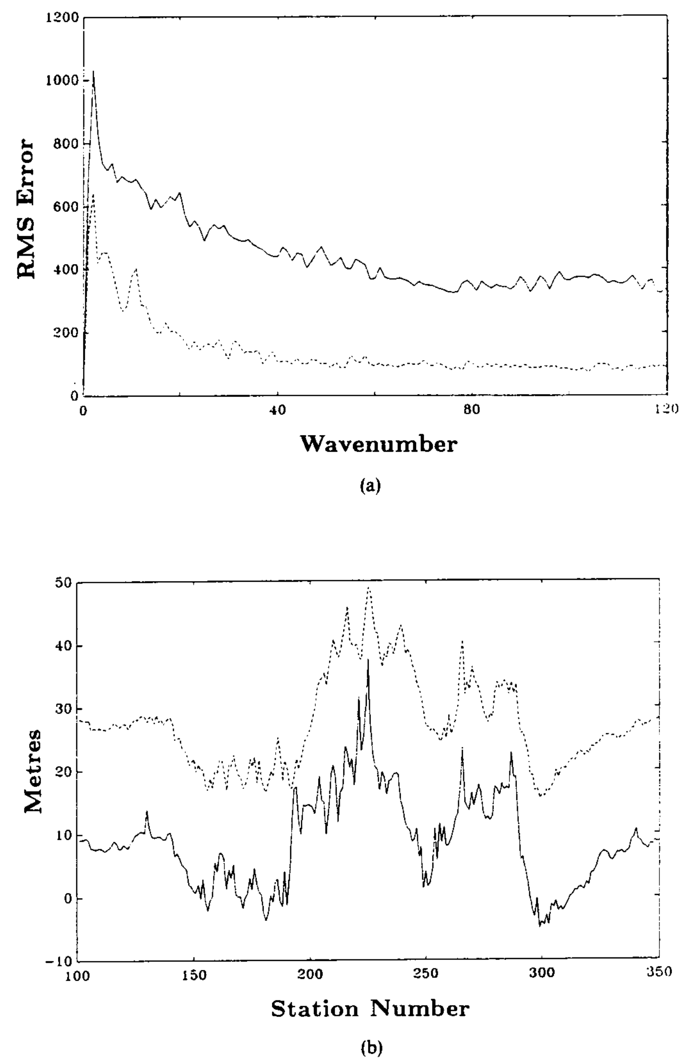

FIG. 13. Results from global inversion of Line 1 in the wavenumber domain. (a) rms-error in wavenumber domain of MER (solid) and adaptive (dashed) picking; (b) values of computed statics; the d.c. difference due to $\Delta\tau_{\text{modelling error}}$ is $\simeq -50$ ms.

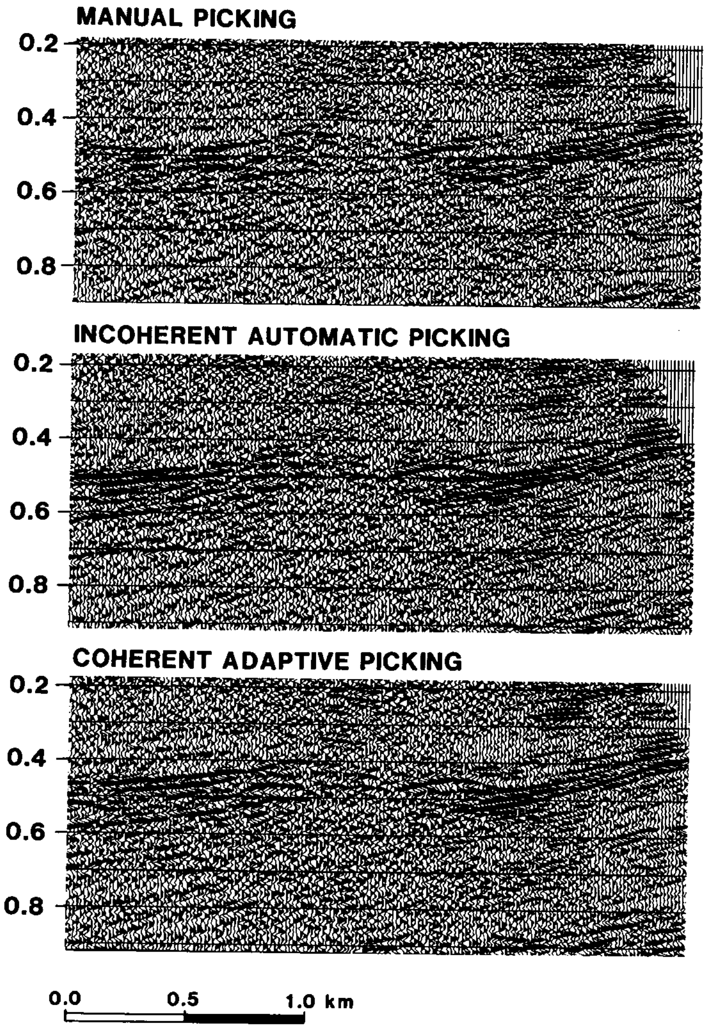

FIG. 14. Stack sections of Line 1 with only refraction static corrections applied.

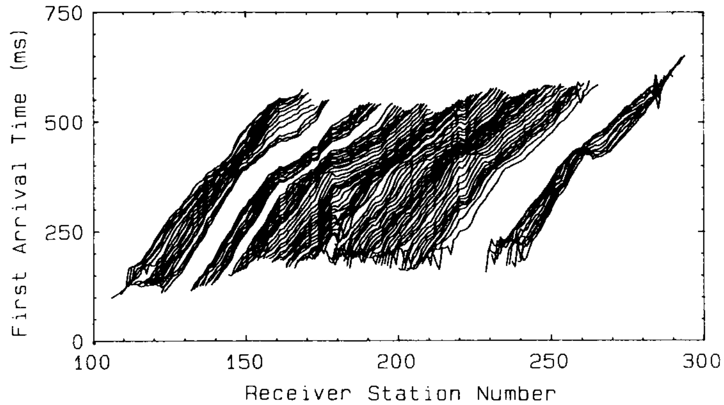

FIG. 15. Traveltime of Line 2 using the adaptive picking.

The matched filter allows the computation of first arrival wavelet parameters consisting of three terms: delay, amplitude and phase shift for every trace. To obtain the wavelet phase in the frequency domain a simple linear approximation ($\theta + \omega\tau$) is used in order to take into account all the causes of phase change with offset.

Using the linear phase approximation, joint and disjoint adaptation achieve the same time resolution, and phase could be only a matching-quality measurement. In a more complex polynomial phase approximation (e.g. quadratic approximation) a disjoint adaptive algorithm controls the phase adaptation more directly to give a complete match. The adaptation rate is controlled by an empirical function (e.g. of cubic form) that has a maximum value dependent on the number of memory iterations.

The accuracy of the first arrival time and phase shift could be improved if a zero-phase deconvolution preceded the picking as follows from the resolution tests.

In conclusion the coherent adaptive picking provides an accurate and fully automatic measurement of first arrival time used in conjunction with amplitude and phase measurements which control the matching-quality.

TABLE 1. Comparison between incoherent and coherent adaptive picking.

	Incoherent picking	Coherent picking
Reliability	Low	High
$\overline{\Delta\tau^2_{noise}}$	High	Low
$\overline{\Delta\tau_{modelling\ error}}$	$\neq 0$	$\simeq 0$
Computer use	Low (1 unit)	High ($\simeq$ 10 units)

Acknowledgements

I thank Professor F. Rocca for many helpful comments and suggestions, AGIP S.p.A. for the field data set and partial financial support.

References

Aki, K. and Richards, P.G. 1980. *Quantitative Seismology: Theory and Methods*. W. H. Freeman and Co.

Angeleri, G.P. 1983. A statistical approach to the extraction of seismic propagating wavelet. *Geophysical Prospecting* **31**, 726–747.

Angeleri, G.P. and Loinger, E. 1984. Phase distortion due to absorption in seismograms and VSP. *Geophysical Prospecting* **32**, 406–424.

Coppens, F. 1985. First arrival picking on common-offset trace collections for automatic estimation of static corrections. *Geophysical Prospecting* **33**, 1212–1231.

Goupillaud, P. 1961. An approach to inverse filtering of near surface layer effects from seismic record. *Geophysics* **21**, 754–760.

Papoulis, A. 1984. *Signal Analysis*. McGraw-Hill Book Co.

Spagnolini, U. 1987. Determinzione dei tempi di arrivo di segnali sismici rifratti. Dissertation for Dr.Ing. degree, Politecnico di Milano.

Taner, M.T., Koehler, F. and Sheriff, R.E. 1979. Complex trace analysis. *Geophysics* **34**, 1041–1063.

Waters, K.H. 1978. *Reflection Seismology*. John Wiley and Sons, Inc.

Woodward, M.J. and Rocca, F. 1988. Wave-equation tomography. 58th SEG meeting, Anaheim, Expanded Abstracts, 1232–1235.

Zanzi, L. and Carlini, A. 1987. Static corrections computation in wavenumber domain. 55th SEG meeting, New Orleans, Expanded Abstracts, 262–265.

Geophysical Prospecting **39**, 313–336, 1991

PRESTACK INVERSION OF GROUP-FILTERED SEISMIC DATA[1]

JAN HELGESEN[2]

Abstract

Helgesen, J. 1991. Prestack inversion of group-filtered seismic data. *Geophysical Prospecting* **39**, 313–336.

Three methods for least-squares inversion of receiver array-filtered seismic data are investigated: (1) point receiver inversion where array effects are neglected; (2) preprocessing of the data with an inverse array filter, followed by point receiver inversion; (3) array inversion, where the array effects are included in the forward modelling.

The methods are tested on synthetic data generated using the acoustic wave equation and a horizontally stratified earth model. It is assumed that the group length and the group interval are identical. For arrays that are shorter than the minimum wavelength of the emitted wavefield, and when the data are appropriately muted, point receiver inversion (first method) gives satisfactory results. For longer arrays, array inversion (third method) should be used.

The failure of the inverse array filter (second method) is due to aliasing problems in the data.

Introduction

Recently there has been an increasing interest in inverse problem theory and methods within the exploration seismic community. A number of papers have treated the problem of non-linear inversion of prestack seismic amplitudes (Tarantola 1984; McAulay 1985; Kolb and Canadas 1986; Kolb, Collino and Lailly 1986; Gauthier, Virieux and Tarantola 1986; Mora 1987; Pan, Phinney and Odom 1988). These authors computed their synthetic traces using *one* receiver per trace. This practice is not fully consistent with today's field data acquisition techniques, where signals from adjacent receivers within a group are added together prior to the recording. Three methods for inverting such array data are presented and tested. The methods are general and can be used in any least-squares inversion scheme based on the wave equation.

[1] Received June 1988, revision accepted September 1990.

[2] Continental Shelf and Petroleum Technology Research Institute A/S, IKU, 7034 Trondheim, Norway.